

Supporting Information

High-Throughput Screening of Stable Layered Anode Materials A_2TMO_3Cl for Chloride-Ion Batteries

Dexing Wang^{a#}, Fusheng Zhang^{a#}, Jianglong Wang^a, Xingqiang Shi^a, Penglai Gong^a, Huanjuan Liu^a,
Mengqi Wu^{a,b,*}, Yingjin Wei^{b,*}, Ruqian Lian^{a,*}

^aKey Laboratory of Optic-Electronic Information and Materials of Hebei Province, National-Local Joint Engineering Laboratory of New Energy Photoelectric Devices, College of Physics Science and Technology, Hebei University, Baoding 071002, P. R. China.

^bKey Laboratory of Physics and Technology for Advanced Batteries (Ministry of Education), College of Physics, Jilin University, Changchun 130012, China.

*Corresponding author:

rqlian@126.com (R. Lian); wumq_jy@163.com (M. Wu)

These authors contributed equally: Dexing Wang, Fusheng Zhang.

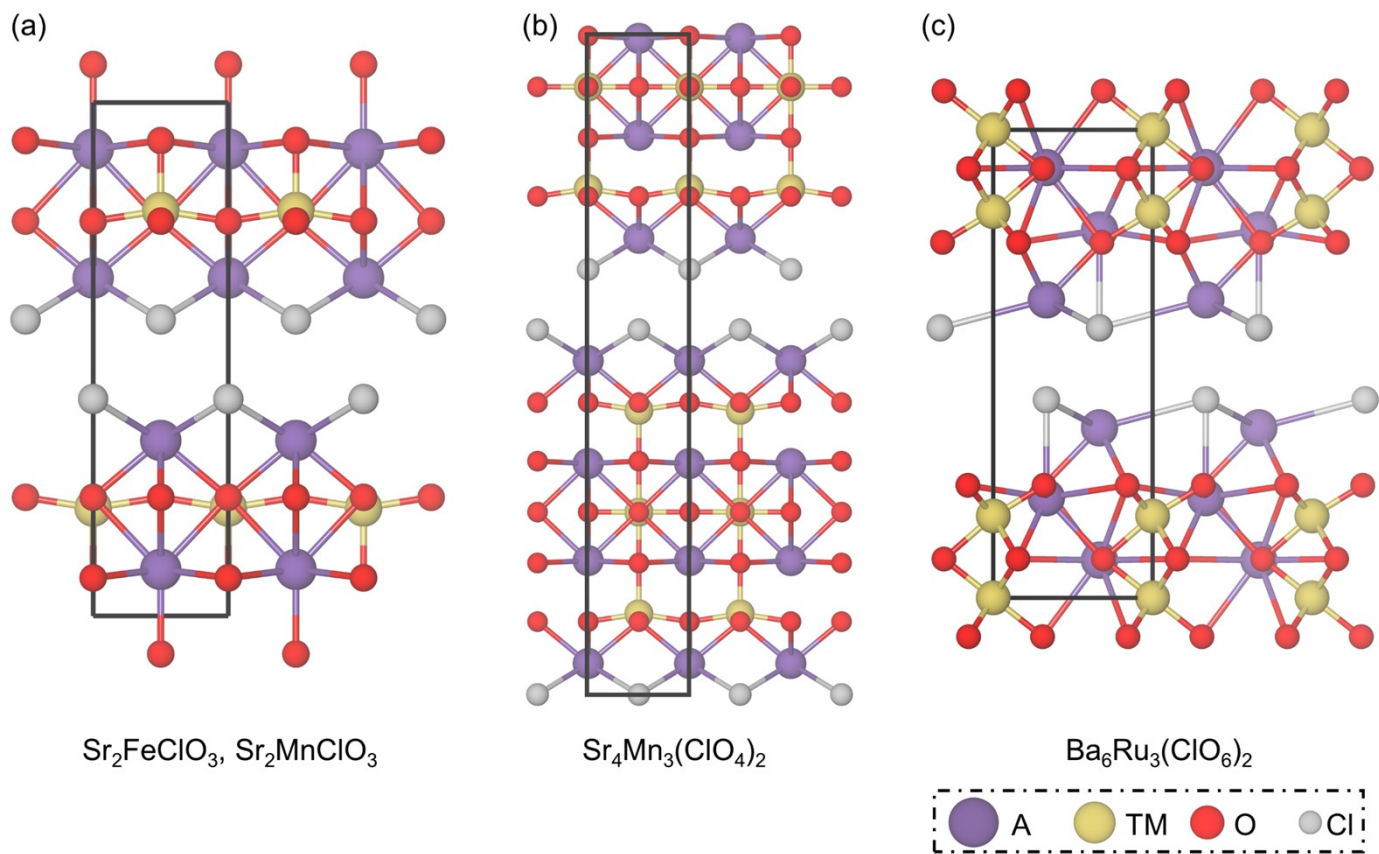
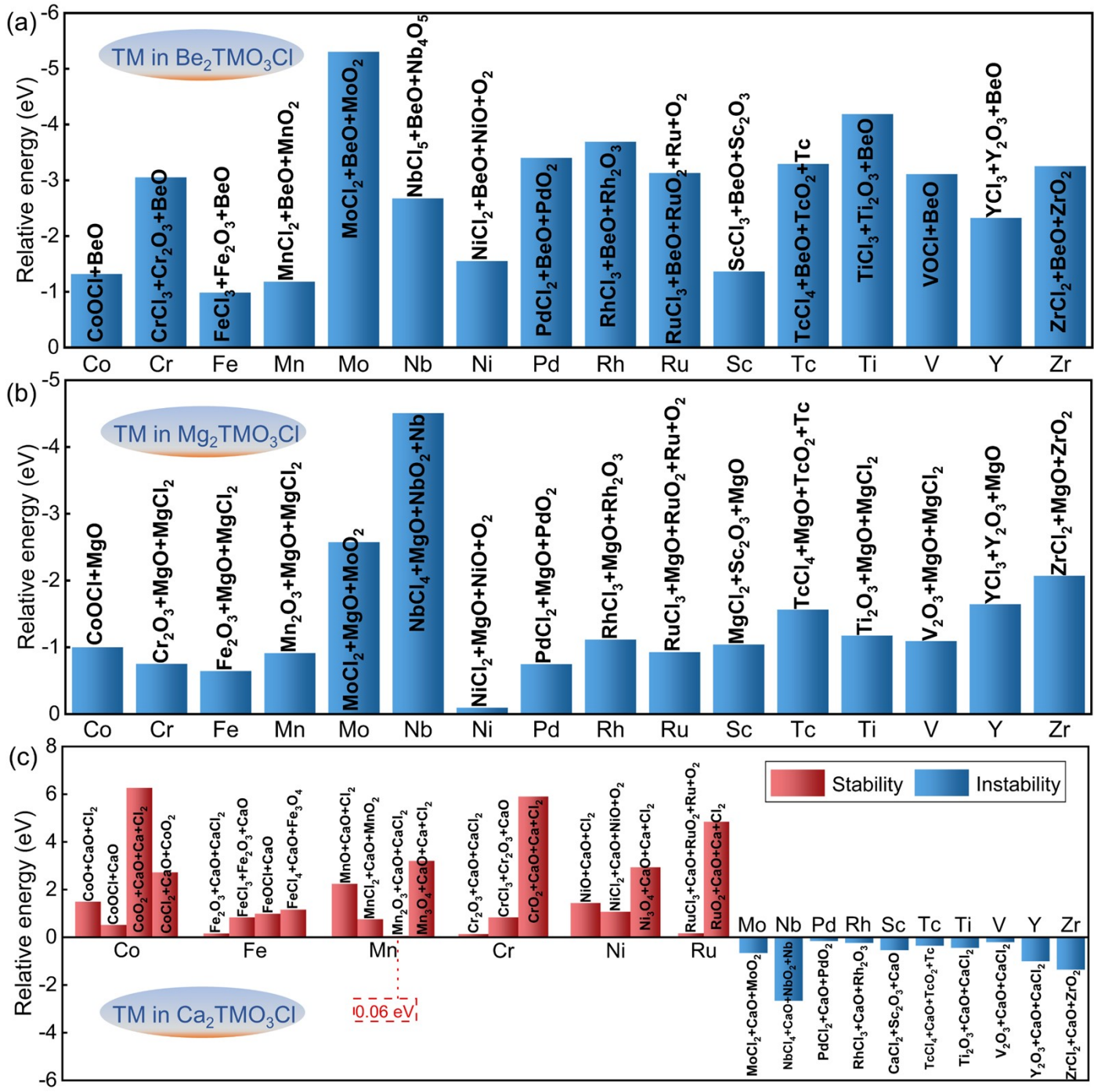


Figure S1. Thermodynamically stable conductive of (a) $\text{Sr}_2\text{FeClO}_3$ and $\text{Sr}_2\text{MnClO}_3$, (b) $\text{Sr}_4\text{Mn}_3(\text{ClO}_4)_2$, and (c) $\text{Ba}_6\text{Ru}(\text{ClO}_6)_2$.



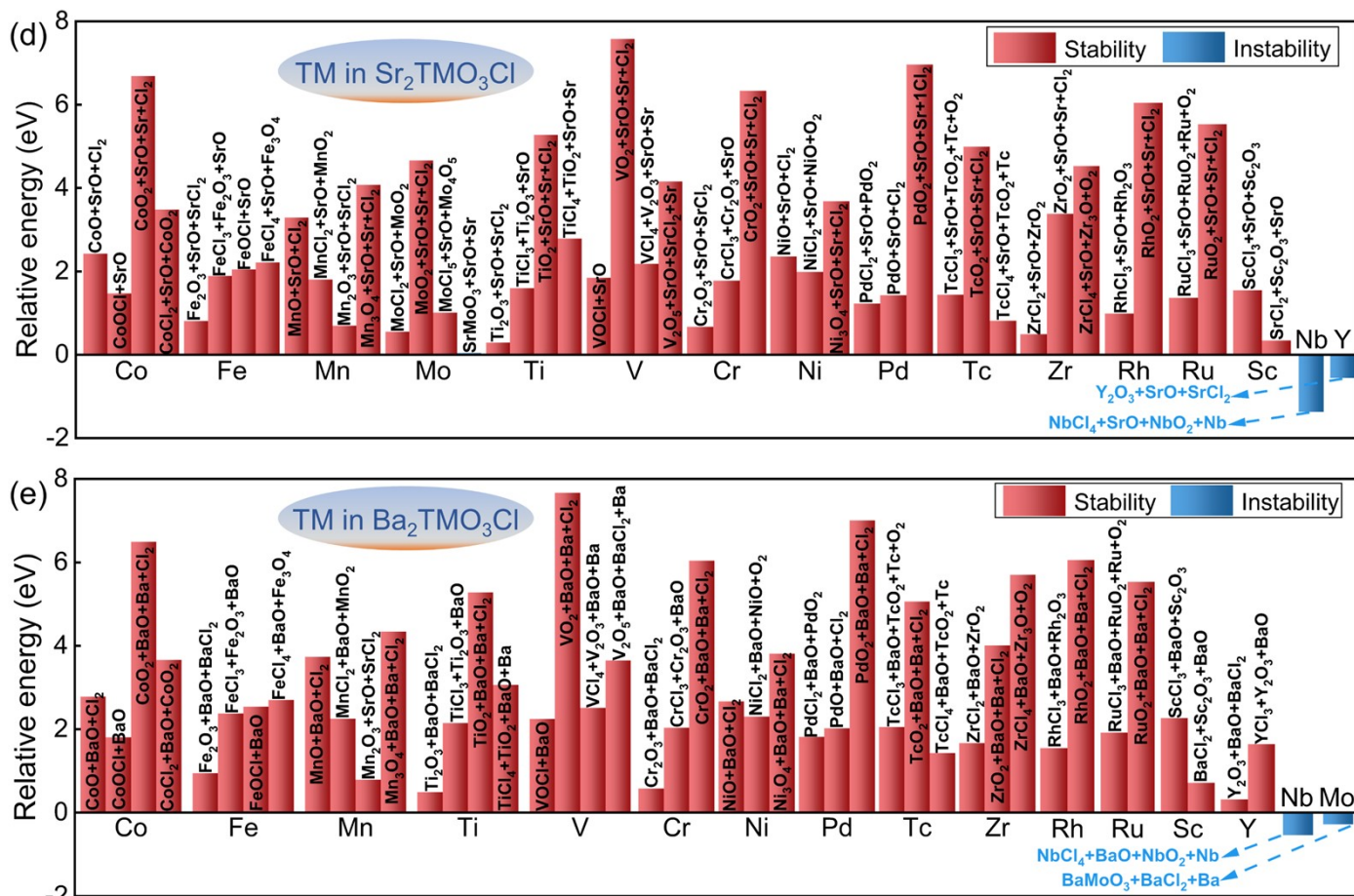
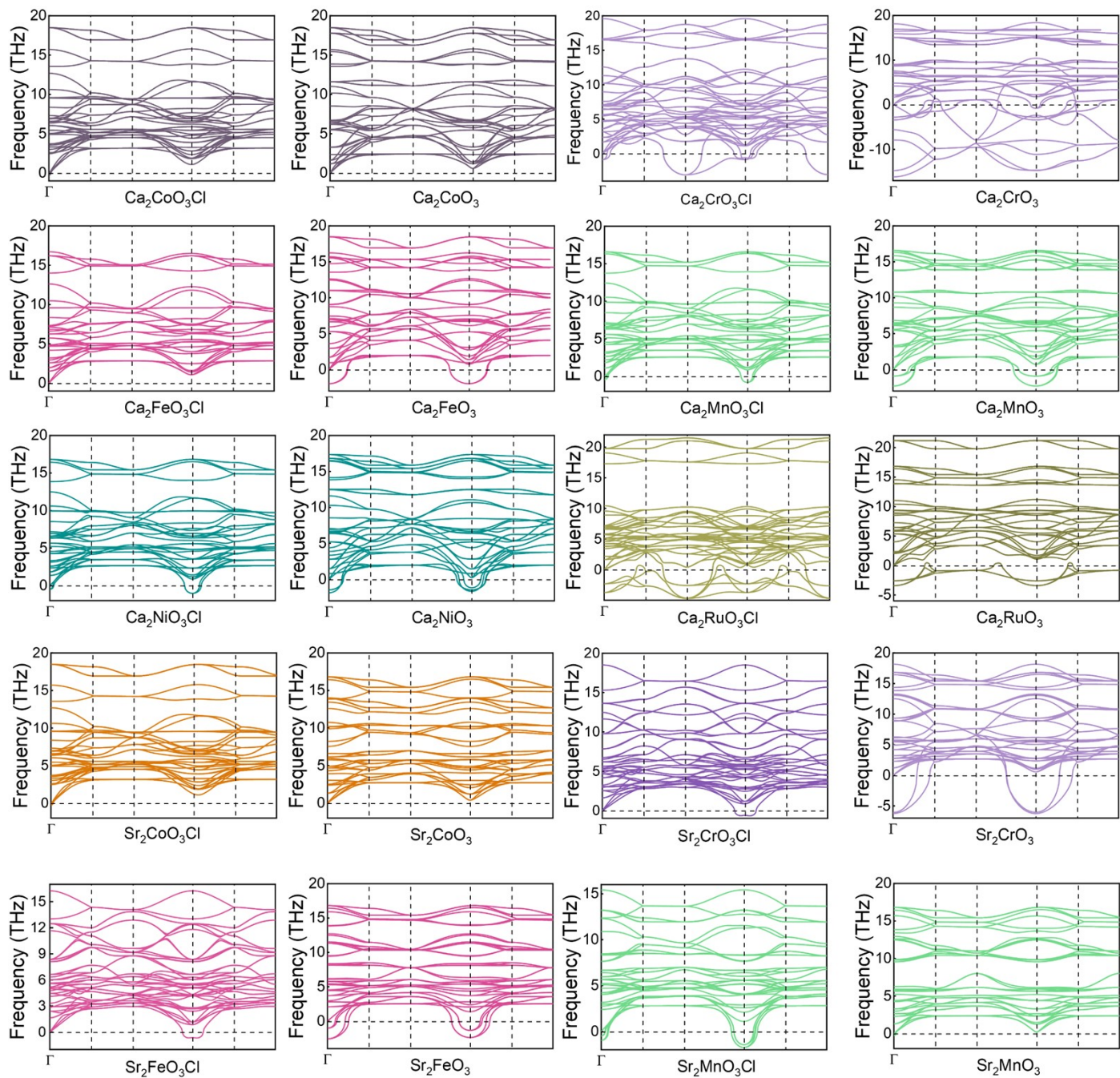
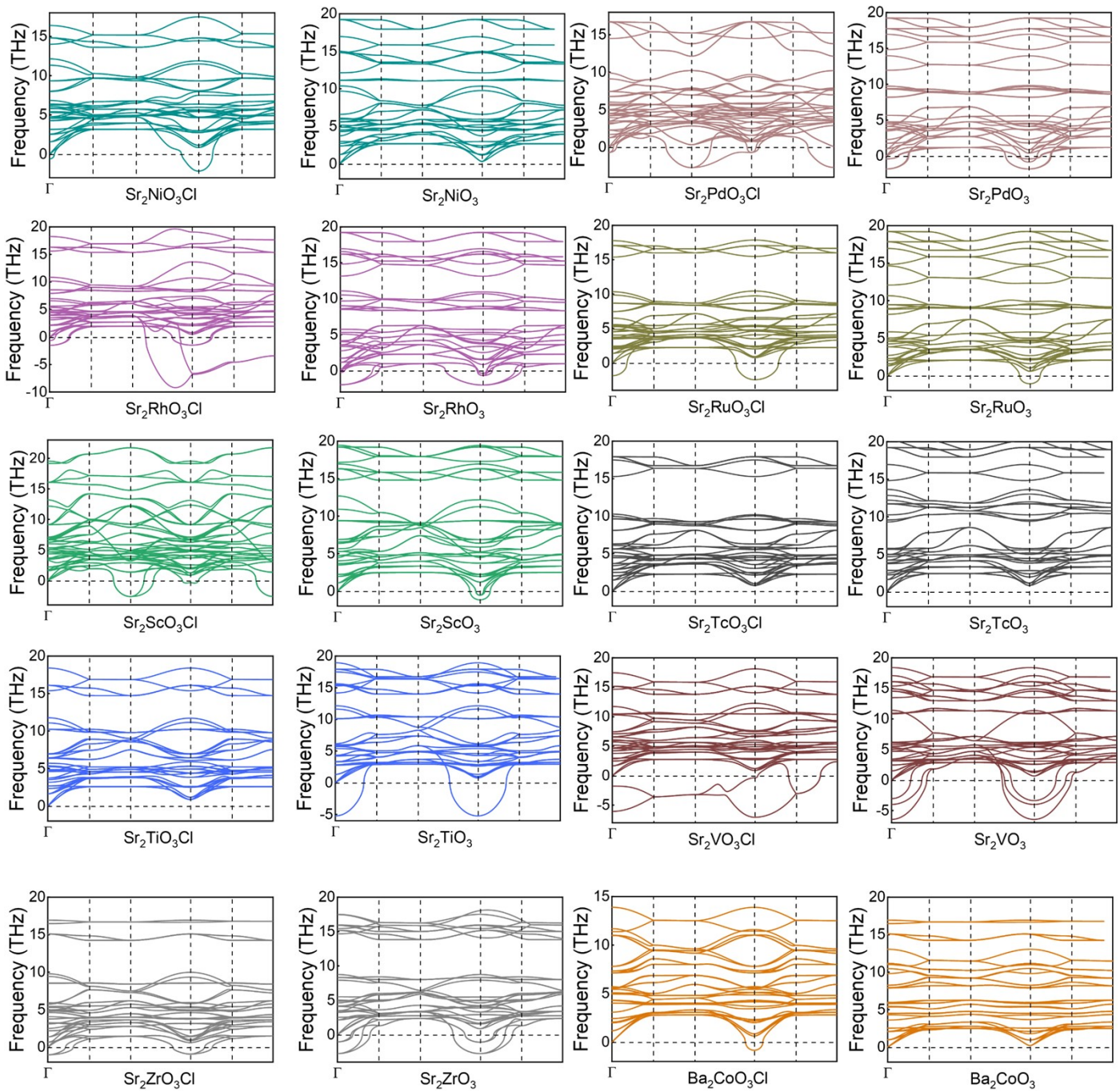
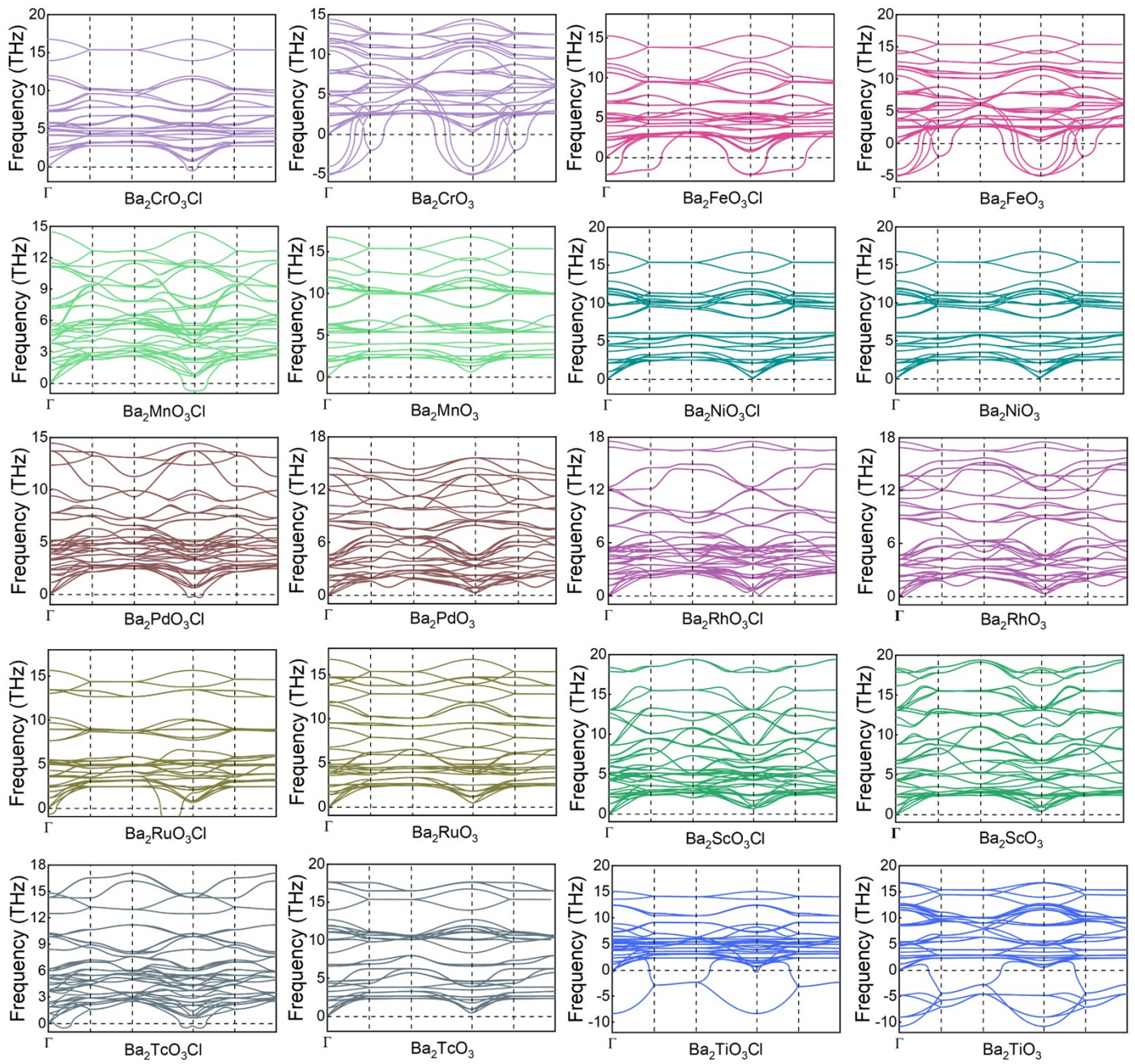


Figure S2. Relative energies between A_2TMO_3Cl and their possible decomposition products. Layered A_2TMO_3Cl are selected as the reference state. ($A = Be, Mg, Ca, Sr, Ba$; $TM = Sc, Ti, V, Cr, Mn, Fe, Co, Ni, Y, Zr, Nb, Mo, Tc, Ru, Rh, Pd$)







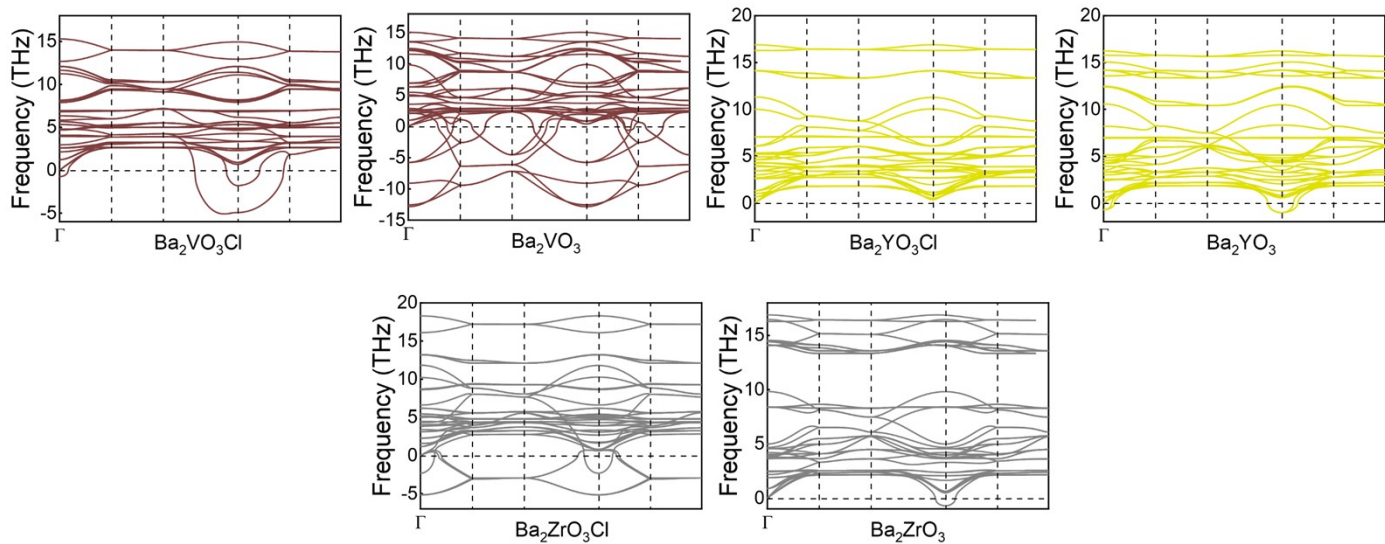


Figure S3. Phonon band structures of thermodynamically stable A_2TMO_3Cl and their dechlorinated states. (A = Ca, TM = Co, Cr, Fe, Mn, Ni, Ru; A = Sr, TM = Co, Cr, Fe, Mn, Ni, Pd, Rh, Ru, Sc, Tc, Ti, V, Zr; A = Ba, TM = Co, Cr, Fe, Mn, Ni, Pd, Rh, Ru, Sc, Tc, Ti, V, Y, Zr).

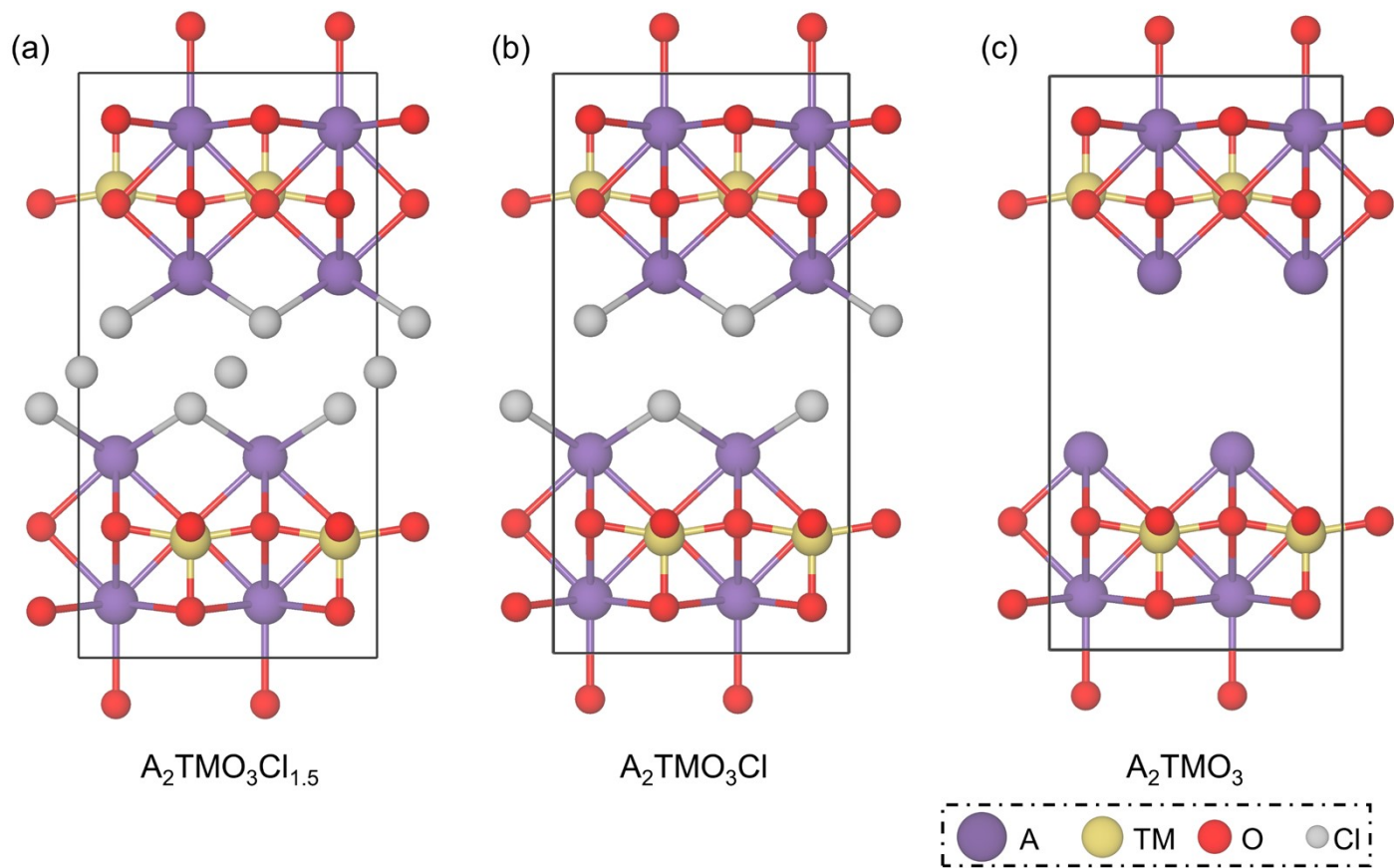


Figure S4. The structures of $A_2TMO_3Cl_x$ at (a) $x = 1.5$, (b) $x = 1$ and (c) $x = 0$.

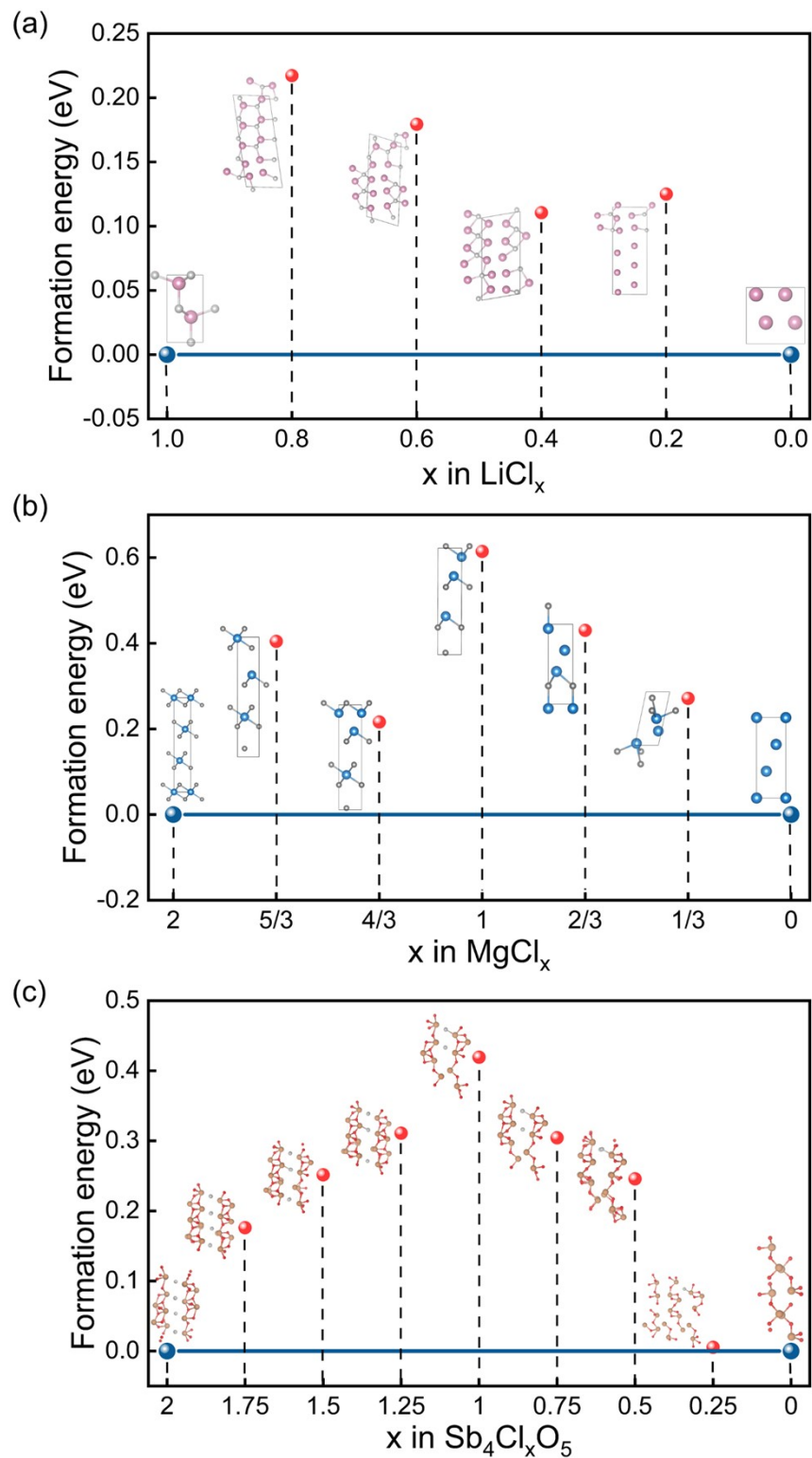


Figure S5. Formation energy of (a) LiCl , (b) MgCl_2 and (c) $\text{Sb}_4\text{Cl}_2\text{O}_5$.

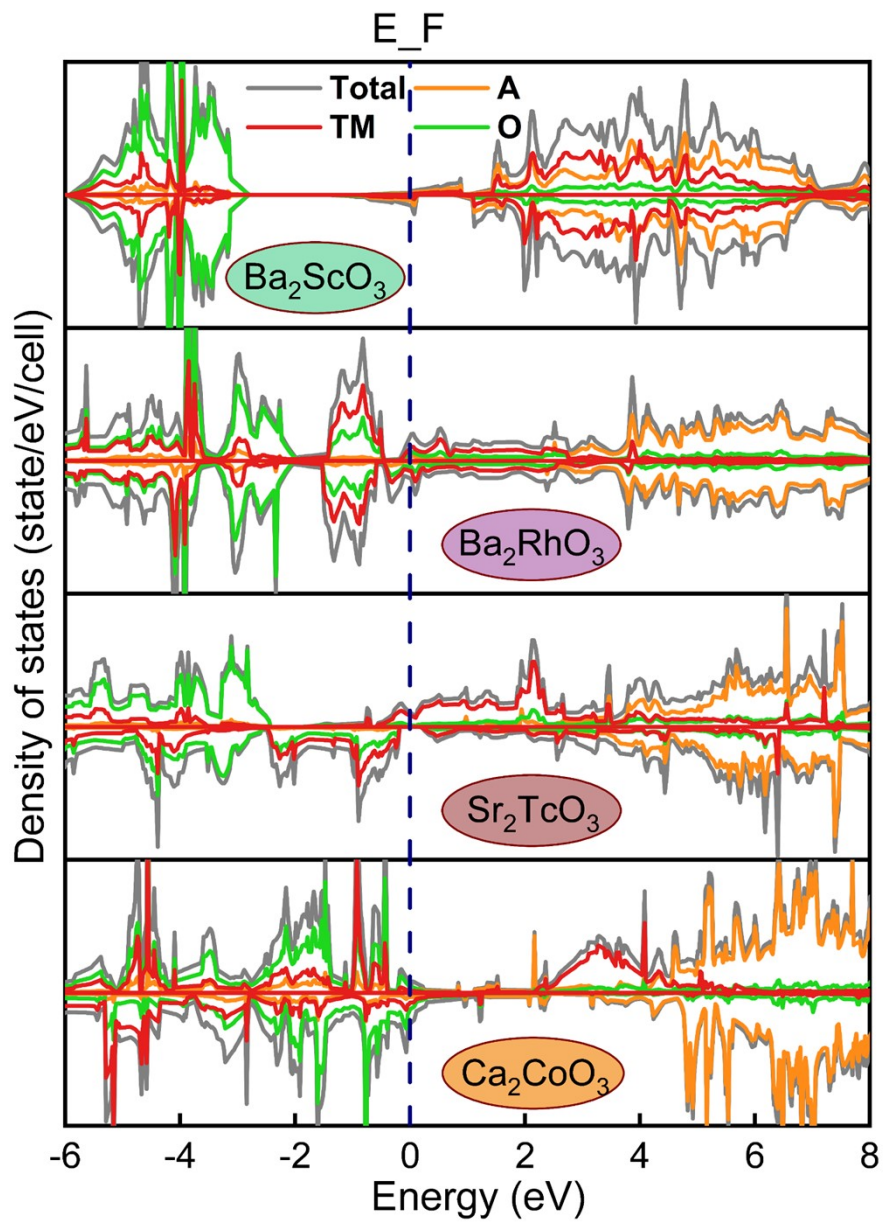


Figure S6. Partial density of states of A, TM, and O (A = Ca, TM = Co; A = Sr, TM = Tc; A = Ba, TM = Sc, Rh)

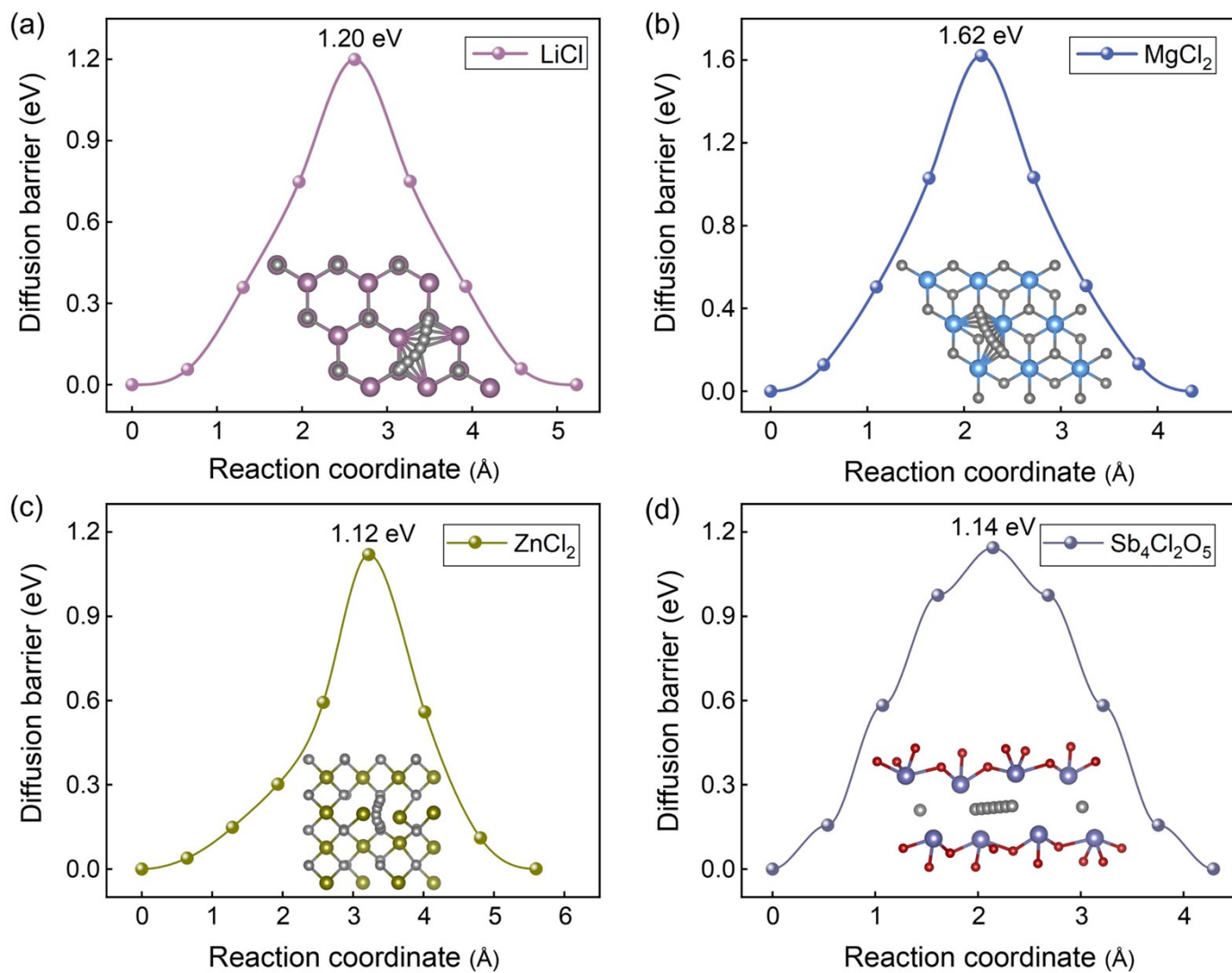


Figure S7. Distribution of Cl⁻ diffusion barrier in reported (a) LiCl, (b) MgCl₂, (c) ZnCl₂, and (d) Sb₄Cl₂O₅.

Table S1. Crystal system, space group, and Cl-layer Observed of thermodynamically stable conductive compounds that containing A, TM, O, and Cl.

Compound	Crystal system	Space group	Cl-layer Observed
$\text{Sr}_2\text{FeClO}_3$	Tetragonal	P4/nmm	Yes
$\text{Sr}_2\text{MnClO}_3$	Tetragonal	P4/nmm	Yes
$\text{Sr}_4\text{Mn}_3(\text{ClO}_4)_2$	Tetragonal	I4/mmm	Yes
$\text{Ba}_6\text{Ru}_3(\text{ClO}_6)_2$	Trigonal	P3m1	Yes
$\text{Rb}_2\text{Pu}(\text{Cl}_2\text{O})_2$	Monoclinic	C12/m1	No
$\text{Cs}_2\text{Pu}(\text{Cl}_2\text{O})_2$	Monoclinic	C12/m1	No
$\text{Sr}_2\text{CrClO}_4$	Orthorhombic	Pbcm	No
$\text{Sr}_2\text{Cu}(\text{ClO})_2$	Tetragonal	I4/mmm	Yes
$\text{Ba}_2\text{Cu}_3(\text{ClO}_2)_2$	Tetragonal	I4/mmm	No
$\text{Ba}_4\text{Os}_6\text{ClO}_{18}$	Cubic	I23	No

Table S2. Bader charge (e) of A, TM, Cl, and O for $\text{Ca}_2\text{CoO}_3(\text{Cl})$, $\text{Sr}_2\text{TcO}_3(\text{Cl})$, $\text{Ba}_2\text{ScO}_3(\text{Cl})$, and $\text{Ba}_2\text{RhO}_3(\text{Cl})$, respectively.

Compound	A	TM	Cl	O
$\text{Ca}_2\text{CoO}_3\text{Cl}$	1.53	1.29	-0.78	-1.19
Ca_2CoO_3	1.32	1.19	-	-1.28
$\text{Sr}_2\text{TcO}_3\text{Cl}$	1.53	1.49	-0.78	-1.25
Sr_2TcO_3	1.38	1.06	-	-1.28
$\text{Ba}_2\text{ScO}_3\text{Cl}$	1.52	1.68	-0.80	-1.31
Ba_2ScO_3	1.40	1.19	-	-1.33
$\text{Ba}_2\text{RhO}_3\text{Cl}$	1.53	1.13	-0.78	-1.13
Ba_2RhO_3	1.48	0.74	-	-1.23